Available online at www.sciencedirect.com
SCIENCE DIRECT®
Solid State Nuclear Magnetic Resonance 28 (2005) 117–124
Solid State Nuclear Magnetic Resonance
www.elsevier.com/locate/ssnmr

Evidence of microphase separation in controlled pore glasses

A. Vyalikh[a], Th. Emmler[a], E. Gedat[a], I. Shenderovich[a], G.H. Findenegg[b], H.-H. Limbach[a], G. Buntkowsky[c,*]

[a]*Freie Universität Berlin, Institut für Chemie, Takustraße 3, 14195 Berlin, Germany*
[b]*Technische Universität Berlin, Stranski-Laboratorium für Physikalische und Theoretische Chemie, Straße des 17. Juni 112, 10623 Berlin, Germany*
[c]*FSU Jena, Institut für Physikalische Chemie, Helmholtzweg 4, 07743 Jena, Germany*

Received 19 June 2005
Available online 1 August 2005

Dedicated to Prof. Dr. Jerzy S. Blicharski, Jagiellonian University in Krakow, Poland, on the occasion of his 65th birthday

Abstract

The phase separation of a mixture of water and isobutyric acid (iBA) confined in the pore space of Controlled Pore Glass (CPG) 10-75 has been studied by ^{1}H NMR relaxometry and ^{1}H-pulsed field gradient (PFG) diffusion measurements. For an acid-rich mixture (mass fraction 54 wt% iBA), evidence of a phase separation process in the pores was obtained, which occurs in a temperature window between 32 and 39 °C, as indicated in the PFG data by an anomalous temperature dependence of the diffusion coefficient and in the relaxation data by a bi-exponential magnetization decay. The phase separation temperature of the mixture in the pore is slightly lower than in the bulk mixture of the same composition (41 °C) and extends over a finite temperature range. A qualitative model of the phase separation process in the pores is developed, which assumes a temperature-dependent domain-like structure of the liquid below the phase transition temperature and a breakdown of these domains upon reaching the transition temperature.

Keywords: Phase separation; NMR diffusometry; Mesoporous silica

1. Introduction

The behavior of fluid molecules in the restricted geometries of mesoporous silica is a matter of current interest [1–4]. Since the physico-chemical properties of the inner surfaces of mesoporous silica can be chemically modified [5,6] mesoporous silica materials are very promising candidates for catalytic applications, which has triggered several recent studies of the dynamics of guest molecules in mesoporous silica [7–10].

In the restricted geometry of the pore the fluid molecules interact with the surfaces, for example, through van der Waals forces of specific interactions such as hydrogen bond interactions. Hence there is a competition between surface–liquid and liquid–liquid interactions. Owing to this competition between surface forces and intermolecular forces the pore fluid may exhibit interesting structures which are often not known for the bulk fluid. For example, the existence of a glass-like phase of benzene inside mesoporous SBA-15 was observed recently [11,12].

For hydrogen bond donor or acceptor molecules, hydrogen bonding plays a major role in the build-up of structures inside the pores, owing to the fact that the silica surface is covered with –SiOH groups, resulting in structures which are expected to be similar to hydration shells of proteins [13,14], or water molecules enclosed in porous solids like zeolites [4] or cements [15]. Recently it was shown that these structures depend crucially on the pore diameter and morphology [16,17]. Even more complex structures than for pure fluids are expected

*Corresponding author. Fax: +49 3641 948302.
E-mail address: gerd.buntkowsky@uni-jena.de (G. Buntkowsky).

0926-2040/$ - see front matter © 2005 Elsevier Inc. All rights reserved.
doi:10.1016/j.ssnmr.2005.07.001

for binary fluid mixtures, which already in the bulk exhibit a complicated phase behavior with temperature- and concentration-dependent regions of miscibility and phase separation [18]. When adsorbed by the porous matrix, the phase separation obviously cannot occur on the macroscopic scale. The question now arises whether two coexisting phases will appear, which might form small domains or a layered coverage of the surface, or whether the interactions with the surface respectively the geometric size restrictions prevent a phase separation.

NMR diffusion measurements are convenient probes for the effects of surface hydrogen bonding and geometric restrictions of fluids inside pores [19–21], owing to the extremely large surface to volume ratio of the mesoporous systems. Since the geometry of the pores is highly anisotropic a preferred axis exists in the direction of the pores' cylinder axis, and diffusion of guest liquids in the pores is expected to exhibit deviations from ordinary diffusion [22,23]. In general, diffusion processes in porous media depend strongly on the type of the host and of the guest molecules. As a result of this dependence, different diffusion models for liquids and fluid guests in porous materials are discussed in the literature for various systems: ordinary diffusion [24,25], restricted diffusion [26,27], anisotropic diffusion [28,29], and diffusion of different phases with individual diffusion coefficients [30]. Ordinary diffusion is well known and describes the behavior of isotropic systems like bulk liquids. Here, the average distribution of mean square displacements is Gaussian and the spin echo intensity decays mono-exponentially with respect to the square of pulsed magnetic field gradient strength.

For heterogeneous systems, such as fluids in porous media, the displacement of the observed molecules depends on interactions with the porous matrix and may be restricted by pore walls. Generally, in such systems, the averaged distribution of mean square displacements is not a Gaussian and, hence, the spin echo attenuation deviates from mono-exponential behavior. Restricted diffusion models were developed for disordered porous systems that are believed to exhibit fractal structure, where the pore walls hinder the guest molecules from free isotropic diffusion. The time dependence of this type of diffusion is described by a power law. Anisotropic diffusion has been studied by NMR for various systems, as for example, water between lamellar layers of a liquid crystal [28], salt water ice [31] or water in MCM-41 [29].

While the behavior of simple liquids inside mesoporous silica are now well characterized and understood, this is not the case for mixtures of several liquids, in particular if these liquids themselves show a complicated phase behavior. Therefore we start to investigate these behaviors, employing a binary mixture of two fluids as the most simple of these systems. For this investigation it is important that the behavior of bulk mixtures is well characterized. We chose to employ the system isobutyric acid (iBA)/water for the following reasons. This system has been used frequently in the literature as a model system in experimental studies of critical phenomena and phase separation in binary liquid mixtures. It can be taken as a representative example of "simple" water-containing systems having a lower miscibility gap (i.e., phase separation occurring at low temperatures—in contrast to systems exhibiting phase separation at elevated temperatures). A water-containing system was chosen in view of the ubiquitous presence of water in nature, but also as a case of a strong preference of the pore wall for one of the components of the mixture. We believe that the chosen system is relevant and representative for a large family of water-containing binary mixtures, and for their behavior in a hydrophilic porous matrix. The phase separation curve of the iBA + D_2O system (Fig. 1) was determined for this work and for the related SANS study (Ref. [41]), where it is shown that our data are in good agreement with literature data by Gansen et al. [32]. The data points in Fig. 1 represent the temperatures at which a mixture of given compositions (weight fraction of iBA) are separating into two phases on slowly cooling the mixture from the one-phase region. A similar coexistence curve for the iBA + H_2O system was determined by several groups in the literature, including Gansen et al. [32]. It is remarkable that replacing H_2O by D_2O causes an upward shift in the critical temperature T_c by nearly 20 K. The system was studied mostly at a bulk composition of 54 wt% iBA. This is a characteristic composition on the iBA-rich side of the critical composition ($w_c = 37$ wt iBA), at which the component preferred by the walls (i.e. water) forms the minority component (always relative to the critical composition). The phase separation of a bulk mixture of 54-wt% iBA is ca. 40 °C. The composition range of 50–60 wt% iBA is of greatest interest as one

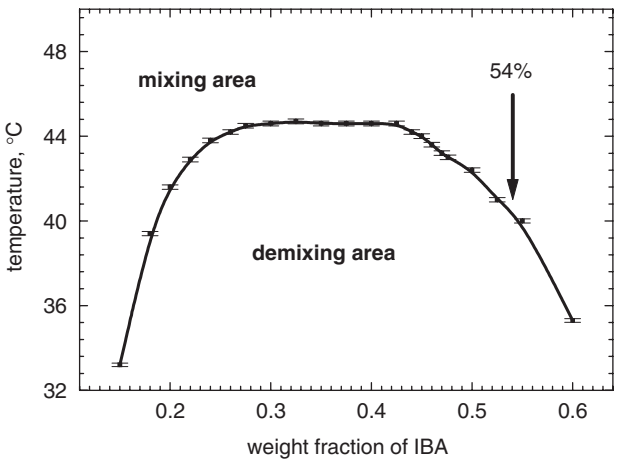

Fig. 1. Phase diagram of the system isobutyric acid plus deuterated water (iBA/D_2O). The arrow marks the composition studied in this work as a guest inside the mesoporous silica.

expects that the microphase separation in the pore will lead to a radial segregation—i.e. formation of a water-rich layer at the pore wall and an iBA-rich core, as is indeed observed. Similar measurements on the water-rich side of the coexistence curve are less rewarding, as the water-rich layer at the pore wall is dominating the behavior and no other features can be seen so clearly. Such a layered structure might even be of relevance to applications of these silica materials in the context of heterogeneous catalysis. In the present work we study the temperature dependencies of translational diffusion and spin–spin relaxation in the iBA/water mixture confined in the mesoporous material Controlled Pore Glass (CPG) 10-75.

The rest of the paper is organized as follows. The materials and techniques used in this study are described in Section 2. The results of the NMR studies as a function of temperature and pore filling for the mixture in CPG 10-75 are presented in Section 3. Finally, in section 4, a model describing the phase transition of the binary mixture in pores is proposed.

2. Experimental section

2.1. Materials and sample preparation

The CPG 10-75 material supplied by Fluka consists of an interconnected pore network with a narrow pore size distribution and an average pore diameter of 10.3 nm. The specific surface area (after Brunauer, Emmett, Teller characterization, BET) of the given batch of CPG 10-75 is $182\,m^2/g$ and the specific pore volume is $0.47\,cm^3/g$. Any organic impurities and physisorbed water in the samples were removed by storing them in concentrated H_2SO_4 for 3 days, followed by Soxhlet extraction with de-ionized water for 2 days and heating to 150 °C in vacuum for 24 h. The CPG was filled into a 5 mm o.d. NMR tube. The tube was heated under vacuum to remove any moisture from the tube walls and the silica and then filled with argon.

For the iBA/D_2O (Deutero, 99.9% deuterated) mixture, we chose a composition of 54 wt% iBA/46 wt% D_2O. The bulk phase behavior of this composition is marked by an arrow in the phase diagram (Fig. 1). The components were initially mixed, then heated to 50 °C and then loaded under an argon atmosphere into the CPG 10-75 inside the NMR tube by a syringe tempered at this temperature. To achieve a complete filling of the pore volume but avoid excess fluid outside the pores, the exact amount of the fluid mixture was calculated from the known pore characteristics (21.7 μl). The sample was kept under an argon atmosphere at room temperature for several hours to reach a saturation of the pores. Then the sample was frozen in liquid nitrogen and flame sealed.

In addition, a sample of CPG 10-75 loaded with pure iBA was prepared for measuring spin–spin relaxation times as a function of the pore filling by stepwise pumping of the guest liquid out of the powder. First, the dried powder sample was weighed and the free pore volume was evaluated, then iBA was loaded using a vacuum line in order to prevent water adsorption from air. Next, the sample was weighed. A pore filling factor V/V_0 (where V_0 is the total pore volume and V is the volume of the confined guest liquid) equal to 0.7 was found. Then stepwise some amount of the iBA was removed from the porous sample at 10^{-6} mbar during several minutes at room temperature for the fully saturated sample and during several hours at 50 °C for the partially filled sample. The heating was done in order to remove the iBA molecules strongly attached to the surface. After each pumping cycle the sample was stored for a few hours at room temperature to achieve thermodynamical equilibrium, accurately weighed and then NMR measurements were carried out. This procedure was repeated until the NMR signals became invisible, which is indicative for the complete desorption of the iBA from the silica.

2.2. Experimental methods

All measurements are carried out on a BRUKER MSL 300 and a VARIAN CMX 300 spectrometer operating at a ^1H resonance frequency of 300.1 MHz in the field of a 7 T wide bore magnet. The magnet is equipped with a vibration damping system, which prevents systematic errors in the determination of the self-diffusion coefficient.

The self-diffusion measurements are performed with a z-shielded gradient probe DSI-747 (Doty Scientific, USA). The pulsed gradient current is delivered by a Techron amplifier, Model 7790 specially designed for gradient NMR. Since the MSL 300 pulse programmer has no analog output, which can be employed as input of the gradient amplifier, a home-built electronic circuit is used, which converts the TTL-pulse from the pulse programmer into an adjustable input signal for the Techron amplifier. The sample temperature is regulated by a Doty temperature controller unit with an absolute error in temperature of ± 1 K. After each diffusion and relaxation measurement the sample temperature was restored to room temperature. The self-diffusion is measured by a stimulated spin–echo pulse sequence ($90°$–τ_1–$90°$–τ_2–$90°$–τ_1–echo). Two rectangular-shaped gradient pulses of duration δ and field strength of $4.00\,T\,m^{-1}$ are applied after the first and third $90°$-RF pulses. The observation time Δ (spacing time between the leading edges of the gradient pulses) was fixed to 12.5 ms. The self-diffusion coefficient D is calculated from the spin–echo intensity attenuation, which is obtained by varying the length δ of the gradient pulse

from 50 to 1400 μs. The raw decay data were corrected with the temperature-dependent contributions of spin–lattice and spin–spin relaxation. The value of the self-diffusion coefficient of water reported by Holz et al. [33] was used for the calibration of the field gradient. A set of measurements at several temperatures was performed and then the averaged value of the gradient coil constant of $0.156 \pm 0.002\,\mathrm{T\,m^{-1}\,A^{-1}}$ was found. All samples were fully thermally relaxed by choosing recycle delays of 3 s. The 90° transmitter pulses were carefully calibrated for all samples and temperatures.

For spin–lattice relaxation time measurements a saturation recovery pulse sequence ($[90°]_n$–τ–90°–FID) was applied. The saturation was achieved with a saturation comb of $n = 51$ pulses. The spin–spin relaxation times were measured by a CPMG sequence ($90°[-\tau-180°-\tau]_n$), typically using 16 values of τ.

2.3. Data processing

Due to the fact that spectra of the mixture inside the pores exhibits only a single broad component, owing to the larger line width, the echo was integrated in the time domain by adding the absolute values of the data (numerical integration). Then the integrated intensities were fed into a laboratory-written Matlab program SIMECAT2 [9] and fitted with normal and two-phase diffusion models to obtain the experimental value of the self-diffusion coefficient.

3. Experimental results

3.1. Self-diffusion measurements

Fig. 2 displays the experimental results of the self-diffusion measurements of the deuterated water/iBA mixture inside the pores at temperatures from 15 to 50 °C. The stimulated spin–echo attenuation curves at different temperatures exhibit clear deviations from an isotropic single-phase diffusion. These deviations are most clearly visible at a temperature of 39 °C, where the fastest echo attenuation, i.e. fastest diffusion, is observed. Interestingly, at temperatures above 39 °C the diffusion gets slower again (see curves at 45 and 50 °C). In addition to this fast decaying component there is a second component visible in the curve, which exhibits a much slower self-diffusion coefficient. According to these results a two-phase diffusion model is employed for the quantitative evaluation of the experimental data. This model assumes the coexistence of two independent non-exchanging phases with separate self-diffusion coefficients. The relative amounts of the two phases, p_1 and p_2, can then be found from the experimental data. This model gives very good agreement between experimental data and fit at all temperatures.

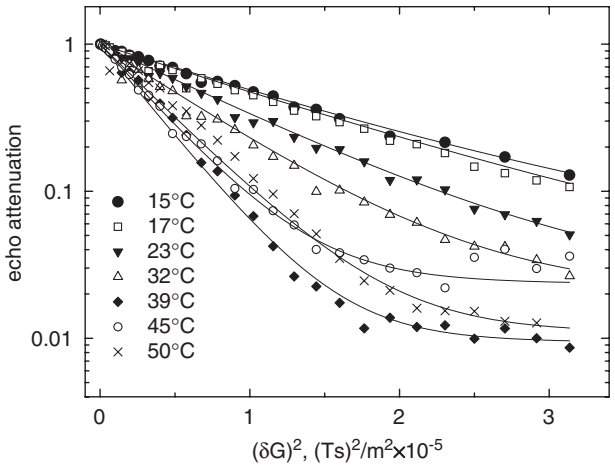

Fig. 2. Experimental and calculated stimulated spin–echo attenuation curves for the system iBA/D_2O confined in CPG 10-75 at different temperatures. The PFG NMR experimental data are indicated by the symbols shown in the insert, the lines represent the fit of the data by the model outlined in the text.

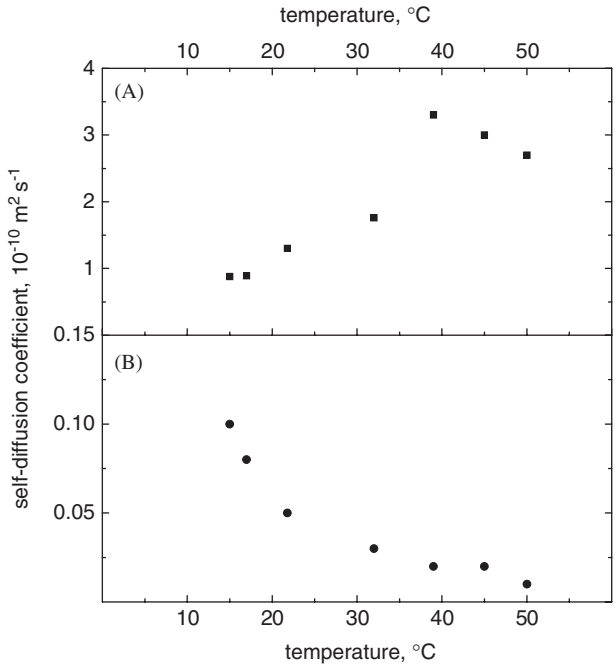

Fig. 3. System iBA/D_2O confined in CPG 10-75: Self-diffusion coefficients D_1 (acid-rich phase, Fig. 6A) and D_2 (water-rich phase, Fig. 6B) as a function of temperature.

The temperature dependence of the resulting diffusion coefficients D_1 and D_2 is presented in Fig. 3. It is found that the phase with the self-diffusion coefficient D_1 is present in great excess. Its relative amount p_1 increases with temperature from 94% to 99%. Accordingly, the relative amount p_2 of the phase with diffusion coefficient D_2 decreases from 6% to 1% in the experimental temperature range. At room temperature self-diffusion of the faster phase is found to be reduced by

approximately one order of magnitude compared to that of bulk components. The second component diffuses even slower. The strongly reduced diffusion coefficient of the mixture components loaded in the pores shows that there is no measurable amount of bulk liquid and all mixture is confined inside the pores, as intended by the sample preparation. The self-diffusion coefficient of the first component increases as the temperature is changed from 10 to 32 °C. A similar temperature behavior, which obeys the Stokes–Einstein equation [34], is observed in bulk ordinary liquids [35,36], bulk mixtures [37] and fluids confined in porous materials [29,38,39]. In the temperature range between 32 and 39 °C the spin–echo attenuation curves as well as the D_1 dependence show a sudden change in their behavior (see Fig. 2 and 3A). After an initial strong increase of the self-diffusion coefficient from 1.8×10^{-10} to $3.3 \times 10^{-10}\,m^2\,s^{-1}$ an anomalous behavior of the self-diffusion coefficient of the acid-rich phase is observed as the self-diffusion coefficient decreases upon further increasing the temperature. As will be discussed in more detail below in the section about the T_2 relaxation measurements, this anomalous slowdown of the translational mobility at increasing temperatures is an indication of a microphase separation in the pores of CPG 10-75.

In contrast to D_1, the diffusion constant D_2 exhibits a continuous decrease with temperature from 10^{-11} to $10^{-12}\,m^2\,s^{-1}$. The relative amount of the two phases does not change significantly over the whole studied temperature range.

3.2. Relaxation measurements

^{1}H spin–lattice T_1 and ^{1}H spin–spin T_2 relaxation times in the confined mixture were measured as a function of temperature. The spin–lattice relaxation curves (not shown) are mono-exponential at all temperatures and only a single common spin–lattice relaxation time for all protons is observed. This common spin–lattice relaxation time exhibits only a slight, non-systematic deviation from its average value of 0.6 s. In contrast, the ^{1}H spin–spin relaxation T_2, shown in Fig. 3, exhibits strong deviations from the mono-exponentiality at temperatures above 39 °C, revealing the presence of two components with different spin–spin relaxation times. While the T_2 decay time of the slower component is temperature dependent, the fast component is nearly temperature independent with a value of ca. 1 ms. This shows that the fast component is an apparent T_2, due to the presence of strong dipolar interactions and not a pure relaxation process. This fact and the presence of slower reorientation rates at the pore surface as well as the ability of water protons or acid carboxyl protons to form hydrogen-bonding to the surface can be used to assign the second component to the surface phase occurring at high temperatures (Fig. 4).

The temperature dependence of the T_2 component with the slower spin–spin relaxation is continuous across the transition point. The semi-logarithmic representation of these values (not shown) indicates a linear increase with reciprocal temperature. These observations lead us to conclude that the spin–spin relaxation times of the first phase results from a single reorientational process with an activation energy of $23\,kJ\,mol^{-1}$. Since the other component is attributed to the surface phase, we attribute this slow component to an inner bulk phase.

In order to reveal the nature of the second phase, which occurs at high temperatures in the T_2 dependence,

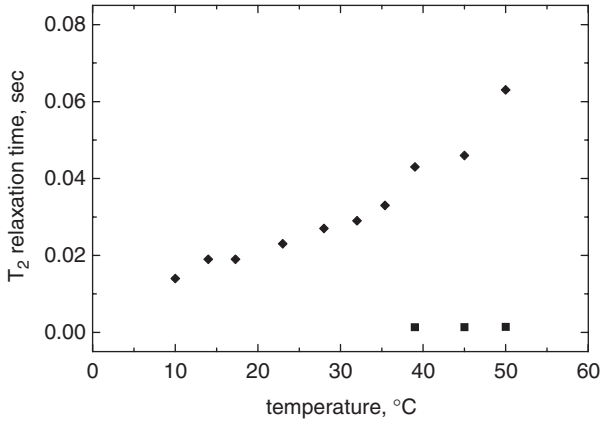

Fig. 4. Temperature dependence of the spin–spin relaxation time T_2 in the confined mixture iBA/D_2O. The squares show the second component of spin–spin relaxation appearing at high temperatures.

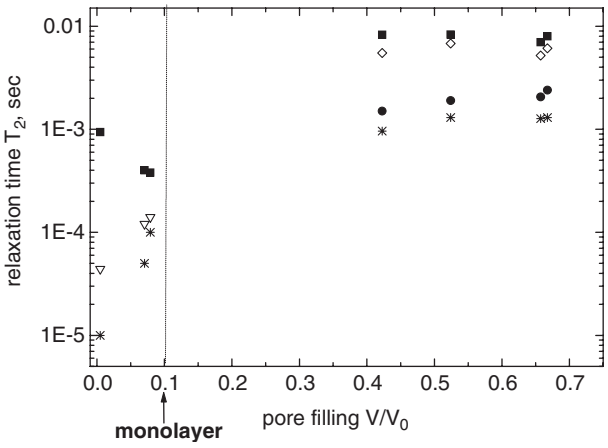

Fig. 5. Spin–spin relaxation times of pure isobutyric acid confined in CPG 10-75 as a function of the degree of pore filling V/V_0. The vertical line indicates monolayer coverage of pore surface as estimated from the geometric characteristics of an isobutyric acid molecule and the CPG 10-75 matrix. Relaxation times of CH_3-groups are indicated by closed squares, CH-groups by diamonds, OH-protons in the core liquid by closed circles, and surface –OH protons by stars and triangles.

the spin–spin relaxation times of iBA molecules confined into the same CPG 10-75 material were measured at different pore saturation degrees. A deconvolution of the NMR signal into contributions from different molecular groups was performed and the T_2 values for each of them were determined. The resulting T_2 data are presented in Fig. 5. A pronounced difference between relaxation times in filled pores (filling factor is from 0.4 to 0.7) and in almost empty pores (filling factor is less then 0.1, which corresponds to a one monolayer surface coverage) is obviously seen. In full pores spin–spin relaxation times are equal to 8 ms for CH_3 and CH groups and ca. 1 ms for both surface and core OH-groups. At low fillings, however, when the molecules are mostly adsorbed on the surface, CH_3 protons are characterized by T_2 relaxation times of 0.4–1 ms and the T_2 values for OH protons are even shorter.

4. Discussion

From the NMR data shown above it is evident that the diffusion rates depend strongly on the temperature. Moreover, above 39 °C the temperature dependence becomes anomalous and a decrease of the diffusion coefficient with increasing temperature is observed.

To understand the results for the confined mixture in the pores, the diffusion coefficients D_1 and D_2 have to be assigned to different protons. Three different assignments were taken into consideration: (i) aliphatic and carboxylic protons of the acid; (ii) water- and acid-rich domains of the confined mixture; (iii) presence of a surface phase and a core phase in the pores. While the first possibility can be ruled out owing to the stoichiometry of the sample, the other two options are feasible. In principle, domain formation and microphase separation in cylindrical pores may lead to two geometries, namely compartmentation in the direction of the pore axis or a radial layer structure. In the former case a strongly restricted diffusion coefficient in the direction of the pore axis is expected. Since this is not observed we conclude that the domains exhibit a network- or layer-like structure. Owing to the hydrophilic nature of the surface silanol groups, a water-rich layer is expected to form at the pore walls so that the acid-enriched liquid is displaced to the core region of the pore space. Accordingly, in the phase-separated state at low temperatures there will be an inner cylinder formed by the acid-rich phase and a cylindrical tube formed by the water-rich phase. Both phases permit free diffusion in the direction of the pore axis. Hence we assume a combination of the second and third options mentioned above by assigning the self-diffusion coefficient D_1 to the acid-enriched liquid (or acid-rich phase) in the core, and D_2 to an adsorbed water-rich layer (or water-rich phase) in contact with the pore walls.

From the NMR experiment one can estimate the mean square displacement of particles diffusing in the direction of the applied gradient during the observation time Δ from Einstein's relation:

$$\langle z^2(\Delta)\rangle = 2D_z\Delta, \tag{1}$$

where D_z is the measured self-diffusion coefficient, assuming that the PFG is applied along the z-axis of the laboratory frame of reference. In three dimensions the total mean square displacement $\langle r^2(\Delta)\rangle$ has to be considered and Einstein's relation leads to the following expression:

$$\langle r^2(\Delta)\rangle = 6D(\Delta)\Delta. \tag{2}$$

From this equation the mean square displacements of molecules at 12.5 ms observation time are estimated to be on the order of a micrometer in the acid-rich phase and of few tenths part of a micrometer in the water-rich phase. The latter value is close to the typical pore length inside the CPG-material, which suggests that the diffusion of the water-rich phase occurs on the surface of the pores. This interpretation is consistent with our qualitative model of the diffusion at higher temperatures (see below), where the strong corrugation of the fluid/fluid interface causes the decrease of the value of the diffusion coefficient and thus the mean square displacement.

As seen in Fig. 3, the acid-rich inner phase exhibits a regular (Stokes–Einstein type) temperature dependence at low temperatures, i.e., the diffusion coefficient D_1 increases with temperature in this regime. The water-rich outer phase with diffusion coefficient D_2 exhibits an inverse temperature dependence, i.e. a slow-down of the diffusion upon increase of temperature. In principle, there are several possible explanations for this anomalous behavior, such as (i) strong exchange of iBA molecules between inner and outer phases across the phase boundary; (ii) an increase of the volume of the diffusing particle with temperature due to the formation of iBA dimers or larger complexes; and (iii) a reduction of the diffusion length, owing to distortions of the structure of the water-rich phase.

The first possibility, which has some similarity with the kinetic model of gas viscosity, can be ruled out because diffusion in the water-rich phase is slower than in the iBA-rich phase. Accordingly, an exchange of iBA molecules with the acid-rich phase would cause an increase and not a decrease of the diffusion coefficient of the water-rich phase in the pores. The second possibility, a slow-down of diffusion due to the formation of iBA dimers or clusters, invokes the concept of hydrophobic aggregation which is entropically driven ($\Delta S > 0$) and thus may cause an enhancement of aggregation with increasing temperature. In the case of iBA such a hydrophobic aggregation is expected to be rather weak, as indicated by the fact that the system iBA/water

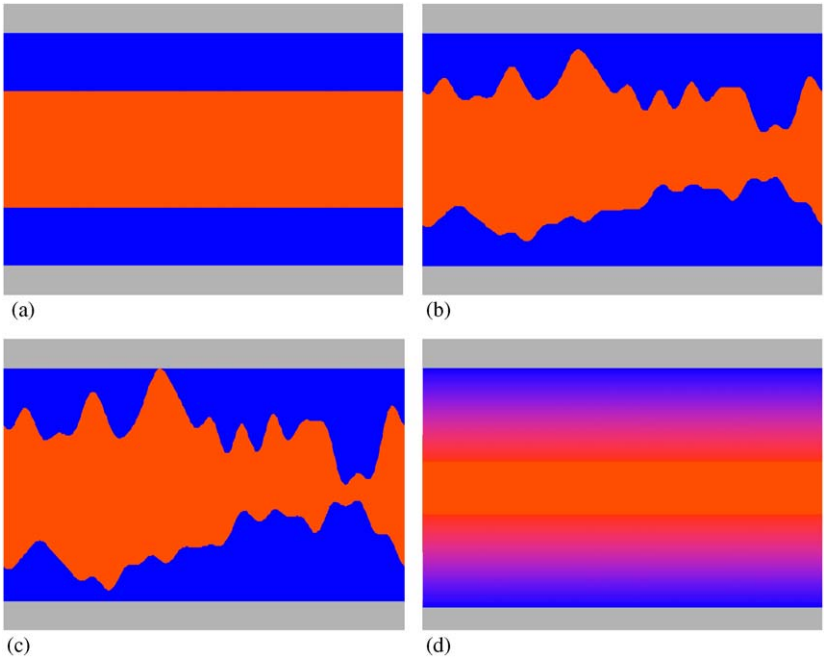

Fig. 6. Sketch of the transition from the phase-separated state (a) to an inhomogeneous one-phase state of the pore liquid (d) as the temperature is increased. In the one-phase region the pore liquid is characterized by a composition gradient from the surface to the center of the pore, due to the preferential adsorption of water at the polar surface.

exhibits not an upper but a lower miscibility gap which is a signature of energy-controlled phase separation. For this reason we believe that hydrophobic aggregation of iBA is not the primary reason for the observed anomalous temperature dependence of the diffusion coefficient D_2.

The main assumption of the third model, sketched in Fig. 6, is that in the phase-separated state of the pore liquid at low temperatures, an increase of temperature causes a reduction of the mean free diffusion pathway in the water-rich phase. It is conjectured that this reduction results from a corrugation of the interface between the water-rich and iBA-rich phases in the pore: whereas at low temperatures the interface between the inner cylinder with the acid-rich phase and a surface layer is rather smooth (Fig. 6a), it becomes corrugated as the temperature is increased (Fig. 6b). For the acid-rich mixture studied in this work the thickness of the water-rich outer layer is rather small and thus a corrugation of the interface will mainly cause a reduction of the diffusion pathway of the molecules in the outer water-rich phase, while the mobility of the acid molecules in the core phase is not strongly affected by this effect. Finally, at temperatures between 32 and 39 °C a transition from the two-phase region to an inhomogeneous one-phase region (characterized by a concentration gradient from the pore wall to the center of the pore (see Fig. 6c) occurs. In the one-phase region the exchange between the water-rich outer and acid-rich inner region starts to dominate. Hence the iBA molecules can easily reach the surface and form hydrogen bonds with the surface silanol groups, which will drastically slow down the diffusion of these bonded iBA molecules. Assuming that the number of hydrogen bonded iBA molecules increases with temperature, this slow-down of the diffusion increases with temperature. This interpretation is supported by the appearance of the second T_2 component at high temperatures, which is attributed to the molecules with low mobility. In other words, this short relaxation time stems from the molecules hydrogen bonded to the surface, which no longer can average out the homonuclear ^{1}H dipolar interaction and thus no longer behave like a liquid but like a solid.

On the basis of this model the total diffusion coefficient above 39 °C is, to a first approximation, the weighted sum of the coefficients from core molecules and molecules bound to the surface, i.e.,

$$D_1 = x_{\mathrm{core}}\, D_{\mathrm{core}} + x_{\mathrm{surf}}\, D_{\mathrm{surf}}, \tag{3}$$

where D_{core} and D_{surf} are the values of the self-diffusion coefficient in the core region and at the surface, and x_{core} and x_{surf} are the relative amounts of the two species. Because of fast exchange at high temperatures on the NMR time scale only the averaged diffusion constant D_1 is observed.

5. Summary and conclusions

In the present work evidence for a microphase separation in the system isobutyric acid (iBA) plus

water confined in the mesopores of Controlled Pore Glass (CPG) 10-75 was found by NMR spectroscopy. The ^{1}H NMR T_2 relaxation time and PFG self-diffusion measurements reveal a transition from the one- to a two-phase region in the pores, which occurs in the temperature range between 32 and 39 °C for the acid-rich mixture (54 wt% iBA) studied in this work. The phase separation in the pore is thus shifted to a lower temperature compared to the phase transition temperature in the bulk mixture of the same composition, which occurs at 41 °C. The combination of the two NMR methods yields the following model of the phase behavior of the confined mixture. At temperatures below the phase transition the pore liquid is separated in microdomains. The molecular mobility in the acid-rich domain which is located in the core region of the pores significantly exceeds the mobility in water-rich domain which forms layer at the pore wall. Upon increasing the temperature the interface between the two phases becomes corrugated. As the phase transition temperature is approached the domains become smaller and the interfaces between them are broadened until the domains transform to concentration fluctuations. At concentration fluctuations on the order of a pore size, the acid molecules in the core phase show the largest mobility. When the temperature is increased above the transition temperature, the number of iBA molecules which can interact with the surface is strongly increased, causing a slow-down of molecular mobility in both phases. The structural model proposed in this work is consistent with a recent study of the local structure of the same system using small-angle neutron scattering [40].

Acknowledgments

This work was supported by the Deutsche Forschungsgemeinschaft through the Sonderforschungsbereich 448 ''Mesoskopisch strukturierte Verbundsysteme''.

References

[1] D.W. Hwang, A.K. Sinha, C.Y. Cheng, T.Y. Yu, L.P. Hwang, J. Phys. Chem. B 105 (2001) 5713.
[2] D.W. Aksnes, L. Gjerdaker, L. Kimtys, K. Foerland, Phys. Chem. Chem. Phys. 5 (2003) 2680.
[3] G. Dosseh, Y. Xia, C. Albe-Simionesco, J. Phys.Chem. 107 (2003) 6445–6453.
[4] E.W. Hansen, M. Stöcker, R. Schmidt, J. Phys. Chem. 100 (1996) 2195–2200.
[5] R. Anwander, I. Nagl, M. Widenmayer, G. Engelhardt, O. Groeger, C. Palm, T. Röser, J. Phys. Chem. B 104 (2000) 3532.
[6] N.T. Whilton, B. Berton, L. Bronstein, H.-P. Hentze, M. Antonietti, Adv. Mater. 11 (1999) 1014.
[7] D.W. Aksnes, L. Gjerdaker, J. Mol. Struct. 27 (1999).
[8] E.W. Hansen, R. Schmidt, M. Stöcker, D. Akporiaye, Microporous Mater. 5 (1995) 143.
[9] E. Gedat, A. Schreiber, G. Findenegg, I. Shenderovich, H.-H. Limbach, G. Buntkowsky, Magn. Res. Chem. 39 (2001) 149.
[10] I. Shenderovich, G. Buntkowsky, A. Schreiber, E. Gedat, S. Sharif, J. Albrecht, N.S. Golubev, G.H. Findenegg, H.H. Limbach, J. Phys. Chem. B 107 (2003) 11924–11939.
[11] E. Gedat, A. Schreiber, J. Albrecht, I. Shenderovich, G. Findenegg, H.-H. Limbach, G. Buntkowsky, J. Phys. Chem. B 106 (2002) 1977.
[12] W. Masierak, T. Emmler, E. Gedat, A. Schreiber, G.H. Findenegg, G. Buntkowsky, J. Phys. Chem. B 108 (49) (2004) 18890–18896.
[13] R. Kimmich, F. Klammler, V.D. Skirda, I.A. Serebrennikova, A.I. Maklakhov, N. Fatkullin, Appl. Magn. Res. 4 (1993) 425.
[14] J. Bodurka, G. Buntkowsky, A. Gutsze, H.-H. Limbach, Appl. Spectrosc. 50 (1996) 1421.
[15] M.J. Setzer, J. Colloid Interface Sci. 243 (2001) 193.
[16] B. Grünberg, T. Emmler, E. Gedat, I. Shenderovich, G.H. Findenegg, H.H. Limbach, G. Buntkowsky, Chemistry 10 (2004) 5689.
[17] J. Trebosc, J.W. Wiench, S. Huh, V.S.Y. Lin, M. Pruski, J. Am. Chem. Soc. 127 (2005) 3057.
[18] L.D. Gelb, K.E. Gubbins, R. Radhakrishnan, M. Sliwinska-Bartkowiak, Rep. Prog. Phys. 62 (1999) 1573.
[19] P.E. Hansen, S. Simon, Magn. Reson. Chem. 35 (1997) 320.
[20] N. Tjandra, A. Bax, J. Am. Chem. Soc. 119 (1997) 8076.
[21] G.S. Kapur, E.J. Cabrita, S. Berger, Tetrahedron Lett. 41 (2000) 7181.
[22] J. Kärger, D.M. Ruthven, Diffusion in Zeolites and Other Microporous Solids, Wiley, New York, 1992.
[23] F.J. Keil, R. Krishna, M.-O. Coppens, Rev. Chem. Eng. 16 (2000) 71.
[24] E.L. Hahn, Phys. Rev. 80 (1950) 580–594.
[25] D.E. Woessner, J. Chem. Phys. 34 (1961) 2057–2061.
[26] R. Kimmich, NMR Tomography Diffusometry Relaxometry, Springer, Berlin, 1997.
[27] J. Kärger, N.-K. Bär, W. Heink, H. Pfeifer, G. Seiffert, Z. Naturforsch. 50a (1994) 186–190.
[28] P.T. Callaghan, Principles of Nuclear Magnetic Resonance Microscopy, Clarendon Press, Oxford, 1991.
[29] F. Stallmach, J. Kärger, C. Krause, M. Jeschke, U. Oberhagemann, J. Am. Chem. Soc. 122 (2000) 9237–9242.
[30] E.W. Hansen, R. Schmidt, M. Stöcker, J. Phys. Chem. 100 (1996) 11396.
[31] M.I. Menzel, S.-I. Han, S. Stapf, B. Blümich, J. Magn. Reson. 143 (2000) 376–381.
[32] P. Gansen, D. Woermann, J. Phys. Chem. 88 (1984) 2655.
[33] M. Holz, S.R. Heil, A. Sacco, Phys. Chem. Chem. Phys. 2 (2000) 4740.
[34] A. Einstein, Z. f. Elektroch. 17 (1908) 235.
[35] W.S. Price, H. Ide, Y. Arata, O. Söderman, J. Phys. Chem. B 104 (2000) 5874.
[36] W.S. Price, H. Ide, Y. Arata, J. Phys. Chem. A 103 (1999) 448.
[37] D.W. Aksnes, L. Kimtys, J. Mol. Struct. 332 (1994) 187.
[38] S. Brandany, M. Jama, D. Ruthven, Microporous Mesoporous Mater. 35 (2000) 283.
[39] D.W. Aksnes, L. Kimtys, Magn. Res. Chem. 36 (1998) 747.
[40] S. Schemmel, G. Rother, H. Eckerlebe, G.H. Findenegg, J. Chem. Phys. (2005), 125, in print.
[41] S. Schemmel, D. Akcakayiran, G. Rother, A. Brûlet, B. Farago, Th. Hellweg, G.H. Findenegg, Eur. Phys. J. E 12 (2003) 1.